Kink effect and noise performance in isolated-gate InAs/AlSb high electron mobility transistors

2012 Semicond. Sci. Technol. 27 065018

(http://iopscience.iop.org/0268-1242/27/6/065018)

Semicond. Sci. Technol. **27** (2012) 065018 (5pp) doi:10.1088/0268-1242/27/6/065018

Kink effect and noise performance in isolated-gate InAs/AlSb high electron mobility transistors

B G Vasallo[1], H Rodilla[2], T González[1], G Moschetti[2], J Grahn[2] and J Mateos[1]

[1] Dpto. Física Aplicada, Universidad de Salamanca, Plaza de la Merced s/n, 37008 Salamanca, Spain
[2] Microwave Electronics Laboratory, Department of Microtechnology and Nanoscience-MC2, Chalmers University of Technology, SE412 Göteborg, Sweden

E-mail: bgvasallo@usal.es

Received 27 February 2012, in final form 24 April 2012
Published 21 May 2012
Online at stacks.iop.org/SST/27/065018

Abstract
The kink effect can spoil the otherwise excellent low noise performance of InAs/AlSb high electron mobility transistors. It has its origin in the pile-up of holes (generated by impact ionization) taking place mainly at the drain side of the buffer, which leads to a reduction of the gate-induced channel depletion and results in a drain current enhancement. Our results indicate that the generation of holes by impact ionization and their further recombination lead to fluctuations in the charge of the hole pile-up, which provoke an important increase in the drain current noise, even when the kink effect is hardly perceptible in the output characteristics.

(Some figures may appear in colour only in the online journal)

I. Introduction

Due to the high mobility of electrons in InAs and the excellent electron confinement in the channel, InAs/AlSb high electron mobility transistors (HEMTs) are being developed for low-power, high-frequency and low-noise applications [1–7]. Nevertheless, these devices present some drawbacks to be eliminated, such as the kink effect (an anomalous increase in the drain current I_D when increasing the drain-to-source voltage V_{DS}), caused by impact ionization and the subsequent hole dynamics in the structure. Impact ionization events are extremely frequent because of the narrow band gap of InAs, and the performance of these devices can be dramatically affected by the kink effect. In particular, it leads to a reduction in the gain and a rise in the level of noise, limiting the utility of these devices for possible microwave or mm-wave applications. Strategies to reduce the negative consequences of the kink effect on the operation of InAs/AlSb HEMTs are thus essential. For example, to overcome the appearance of the associated excessive gate leakage current related to impact ionization-generated holes, the conventional Schottky contact has been replaced by an isolated gate by means of a native oxide [7]. However, the reduction of the kink effect-related noise is still an issue.

The purpose of this work is to analyze the influence of the kink effect on the noise performance of isolated-gate InAs/AlSb HEMTs. With this aim, we make use of a semiclassical 2D ensemble Monte Carlo (MC) simulator [8] adequately adapted to correctly reproduce the experimental static, dynamic and noise behavior of InAs/AlSb devices in the absence of the kink effect (i.e. for low values of V_{DS}) [9–11], in which the impact ionization and hole transport have been included [12–14]. The MC method is the most appropriate technique for the analysis of these devices, since electron transport can easily turn into ballistic or quasi-ballistic in the channel due to the huge mobility of InAs [9]. Moreover, with our MC method, a complete physical understanding of the kink phenomenon and its influence on the noise behavior in these devices can be achieved, thus providing helpful information for the development of Sb HEMTs with improved immunity to this effect.

The paper is organized as follows. In section 2 the physical model is detailed. The main results and their discussion are provided in section 3. Finally, in section 4, we draw the most important conclusions of this work.

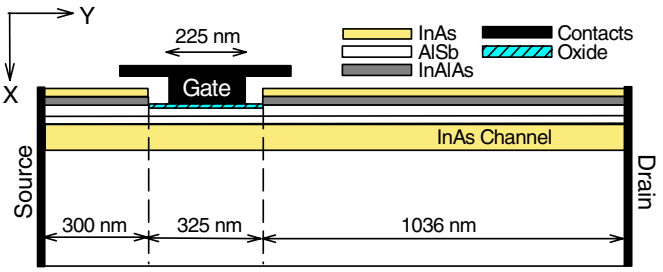

Figure 1. Schematic topology of the HEMT under analysis.

2. Physical model

For the calculations we make use of an ensemble MC simulator self-consistently coupled with a 2D Poisson solver which incorporates the processes at the origin of the kink effect. The simulated structure is very similar to the experimental one described in [6], which has been used to calibrate our model by reproducing the static characteristics. The structure under analysis is a 225 nm T-gate-recessed HEMT (figure 1), fabricated on a heterostructure consisting of an InP substrate (not simulated), an 800 nm AlSb buffer followed by a 15 nm thick InAs channel, two layers of AlSb (a 5 nm spacer and a 10 nm Schottky layer, separated by a 5×10^{12} cm^{-2} δ-doped layer), and, finally, a 4 nm thick AlInAs and 5 nm thick InAs cap layer ($N_D = 5 \times 10^{18}$ cm^{-3}). The MC parameters for the electron transport simulation in the involved materials can be found in [9].

In the MC simulations, impact ionization is included for electrons in the Γvalley by means of the Keldysh approach [15]: the probability per unit time of having an impact ionization event is given by $P(E) = S[(E - E_{th})/E_{th}]^2$ if $E > E_{th}$ and $P(E) = 0$ if $E < E_{th}$, E being the electron kinetic energy in the Γ valley, E_{th} the ionization threshold energy and S a measure of the softness or hardness of the threshold. When an impact ionization process takes place, a hole in the heavy-hole valence band and an electron in the Γ valley emerge, while the original electron remains in the Γ valley. All the details for the modeling of hole transport can be found in [14].

For a proper analysis of the kink effect, hole recombination must also be taken into account. Therefore, we use a simple model in which hole recombination is considered to take place with a characteristic time τ_{rec} (i.e. with a probability $1/\tau_{rec}$). We have performed simulations with $\tau_{rec} =$ 0.05 ns, since with this value of τ_{rec} (jointly with those of E_{th} and S) the experimental static output characteristics are adequately reproduced [14]. Moreover, we have considered other values of τ_{rec} in order to check its influence on the noise behavior of the device.

Regarding the noise calculations, the fluctuations of the current flow through the drain electrode are studied by means of the autocorrelation function. The corresponding spectral density of drain current fluctuations is determined by the Fourier transform of the mentioned autocorrelation function [13]. Due to the presence of the isolated gate, the gate current and thus the corresponding noise performance are extremely low for a proper analysis with our MC model.

3. Results and discussion

Figure 2 shows the simulated (*a*), (*b*) extrinsic and (*c*), (*d*) intrinsic *I*-*V* characteristics of the InAs HEMT in the presence and absence of impact ionization. In figures 2(*a*) and (*b*), the experimental *I*–*V* curves [7] have been included for comparison, and in figures 2(*c*) and (*d*) the case of $\tau_{rec} = 0.02$ ns has been added to check the influence of the recombination time on the static characteristics. In order to carry out the comparison of the measured results (extrinsic) with those obtained from the simulation (intrinsic), drain and source parasitic resistances, associated with metallizations and part of the ohmic regions not included in the simulation domain, have been incorporated into the original MC results. The best fit has been obtained for $R_S = 0.13$ Ω mm and $R_D = 0.38$ Ω mm [9, 14]. Remarkable agreement between experimental and simulated results is reached when considering impact ionization in the simulations with values for the involved parameters of $E_{th} = 0.41$ eV, $S = 10^{12}$ s^{-1} and $\tau_{rec} = 0.05$ ns, as mentioned previously. A notable increase in I_D takes place starting from a value of V_{DS} high enough for the onset of impact ionization (about $V_{DS} = 0.3$ V, figure 2(*b*)), leading to a threshold voltage shift at high V_{DS} (figure 2(*a*)). The relative increase in I_D with respect to the case of the absence of impact ionization is smaller for a shorter recombination time (figures 2(*c*) and (*d*)).

MC simulations provide an insight into the microscopic processes taking place inside the devices, in terms of which the kink effect has been explained. Figure 3 shows the potential profile along the channel near the spacer (*a*), near the buffer (*b*) and the sheet electron density with and without considering impact ionization in the simulation (*c*) for $\tau_{rec} = 0.05$ ns, $V_{DS} = 0.4$ V and $V_{GS} = -0.6$ V. Holes generated by impact ionization in the drain region of the channel (where the electric field, and consequently the electron energy, is higher) accumulate mostly at the drain side of the buffer, which leads to the difference in the channel potential profile with respect to the case of the absence of impact ionization, as observed in figures 3(*a*) and (*b*). This occurs because most of the generated holes descend the energy step present in the valence band at the heterojunction between the InAs channel and the AlSb buffer. Then, the energy of the holes decreases due to scattering mechanisms, so that the attracting force of the gate potential and the negative surface charge at the recess are not sufficient for them to surmount back the energy barrier in the valence band and thus return to the channel. This pile-up of positive charge lowers the potential barrier that controls the current through the channel, mainly near the buffer side (figures 3(*a*) and (*b*)), so that the channel is further opened, with the consequent increase in the electron density (figure 3(*c*)) and drain current. The rise in I_D is basically due to this enhancement in the electron flow through the channel, since the number of electrons/holes generated by impact ionization is very low so as to provide a significant contribution to I_D.

The kink effect is a source of excess noise. The generation of holes by impact ionization and their further recombination lead to fluctuations in the pile-up of positive charge located in

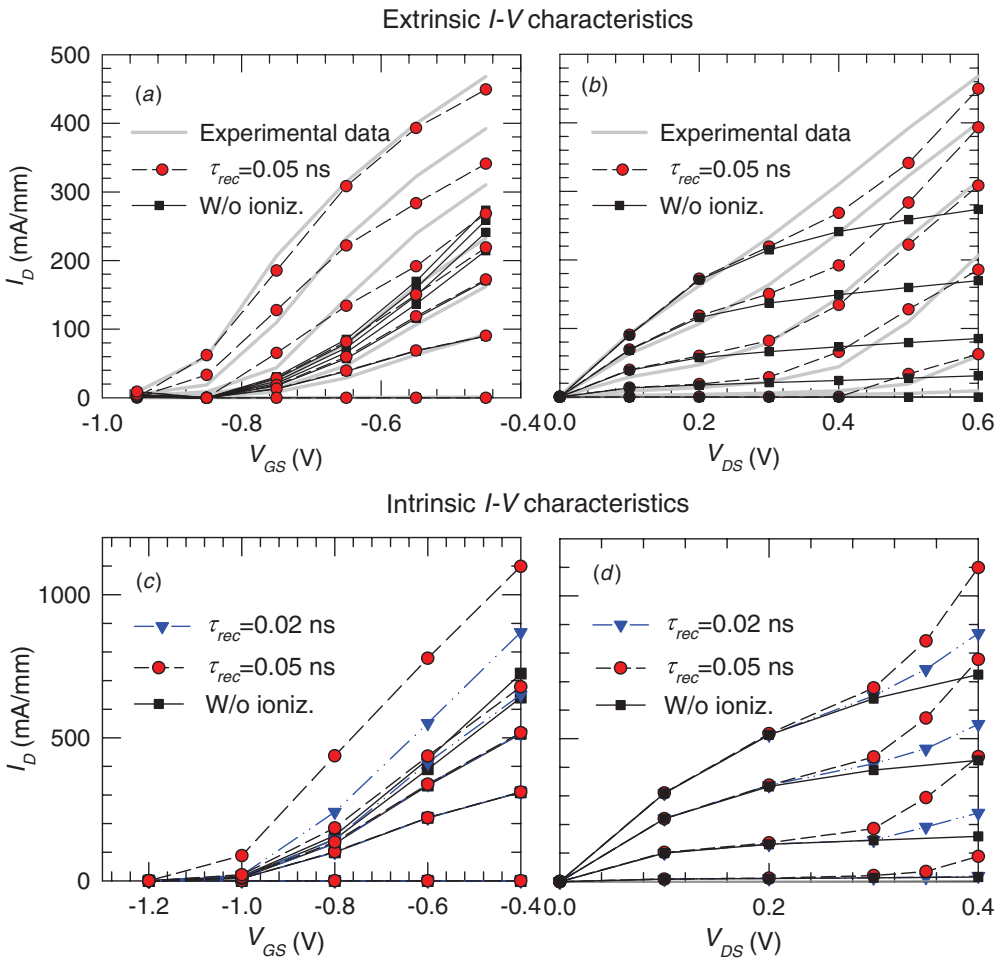

Figure 2. MC (*a*), (*b*) extrinsic and (*c*), (*d*) intrinsic *I*--*V* characteristics for the InAs/AlSb HEMT in the presence and absence of impact ionization, with $E_{\rm th} = 0.41$ eV, $S = 10^{12}$ s^{-1} and different $\tau_{\rm rec}$. Experimental results of the similar fabricated structure are plotted in (*a*) and (*b*) for comparison. In the $I_{\rm D}$–$V_{\rm GS}$ curves, $V_{\rm DS}$ is (*a*) 0.6 V and (*c*) 0.4 V for the top curves, and the potential step is $\Delta V_{\rm DS} = -0.1$ V in both cases. In the $I_{\rm D}$–$V_{\rm DS}$ curves, $V_{\rm GS}$ is (*b*) −0.45 V and (*d*) −0.40 V for the top curves, and the potential step is (*b*) $\Delta V_{\rm GS} = -0.1$ V and (*d*) $\Delta V_{\rm GS} = -0.2$ V.

the buffer of the device. These charge fluctuations are strongly coupled to the drain current by the induced fluctuations on the potential barrier that controls the transport of electrons through the channel. Thus, an important increase in the drain current noise is expected to take place concurrently with the kink in the $I_{\rm D}$–$V_{\rm DS}$ curves. The cutoff of this excess noise should thus be related to the relaxation time of the hole accumulation fluctuations.

Figure 4 shows the spectral density of drain current fluctuations $S_{\rm ID}(f)$ in the presence and absence of impact ionization, for (*a*) $V_{\rm DS} = 0.4$ V, $\tau_{\rm rec} = 0.05$ ns and different $V_{\rm GS}$, and for (*b*) $V_{\rm GS} = -0.4$ V, $V_{\rm DS} = 0.4$ V and different $\tau_{\rm rec}$. Both impact ionization and hole recombination lead to a positive long-time contribution in the drain current correlation function, which causes a significant increase in the low-frequency plateau in $S_{\rm ID}(f)$, which is not present when impact ionization is removed from the simulations. The characteristic cutoff frequency of the plateau in $S_{\rm ID}(f)$ is linked to the impact ionization rate and the hole recombination probability, this being $1/\tau_{\rm rec}$. Moreover, the longer the $\tau_{\rm rec}$, the higher is the noise level. At frequencies beyond the cutoff, the noise remains practically independent of $\tau_{\rm rec}$, exhibiting the typical peak related to plasma oscillations in the highly doped regions of the structure. For the case in which $\tau_{\rm rec} = 0.05$ ns the drain current autocorrelation function has a very long-time tail, which leads to spurious mathematical contributions to the $S_{\rm ID}(f)$ curve, which must not be taken into account for the global explanation [13]. Note that in the case of the absence of impact ionization the low-frequency plateau shows no cutoff before the noise increase related to plasma oscillations.

The low-frequency value of the spectral density of drain current fluctuations $S_{\rm ID}(0)$ is presented in figure 5 as a function of (*a*) $V_{\rm GS}$ for $V_{\rm DS} = 0.4$ V and (*b*) $V_{\rm DS}$ for $V_{\rm GS} = -0.6$ V, for different values of $\tau_{\rm rec}$. The case of the absence of impact ionization is also included for comparison. $S_{\rm ID}(0)$ is found to increase with $V_{\rm DS}$ due to higher current and number of impact ionization events taking place at a larger gate–drain potential difference. The increase in $S_{\rm ID}(0)$ is especially pronounced for high $V_{\rm GS}$. This is the opposite behavior to that found for InGaAs/InAlAs HEMTs [10], where, when the channel is opened, the maximum electron energy, and thus the number of impact ionization events, is reduced due to the lower gate-to-drain potential (although the electron density in the channel is larger). In the case of InAs/AlSb HEMTs, the band gap of the

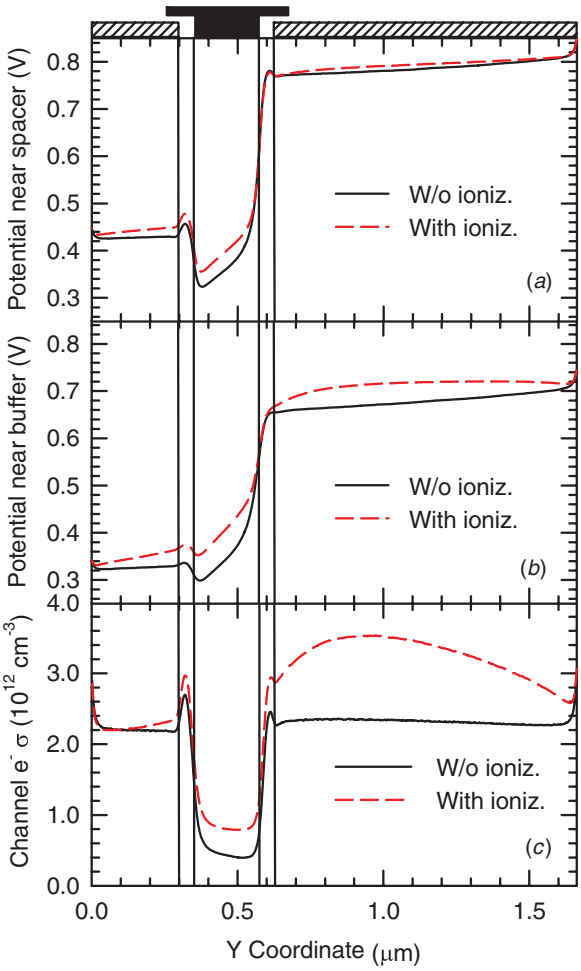

Figure 3. MC profiles along the channel of (*a*) potential near the spacer and (*b*) potential near the buffer, and (*c*) the sheet electron density with and without considering impact ionization in the simulation, with $V_{DS} = 0.4$ V, $V_{GS} = -0.6$ V. $E_{th} = 0.41$ eV, $S = 10^{12}$ s^{-1} and $\tau_{rec} = 0.05$ ns.

channel material and also the threshold energy E_{th} are much smaller than for InGaAs/InAlAs devices, so that the impact ionization probability remains significant for higher values of V_{GS}. Furthermore, impact ionization events take place not only near the maximum of electron energy (under the gate electrode) but all along the drain side of the channel, where the electron velocity is higher when increasing V_{GS}. This leads to higher values of I_D and, thus, $S_{ID}(0)$ when increasing V_{GS}. Moreover, the values of $S_{ID}(0)$ are larger for higher τ_{rec} due to the longer time for which holes remain inside the device before recombination, which leads to a higher hole density and a longer characteristic time of hole density relaxation.

As observed in figure 5, $S_{ID}(0)$ depends on V_{DS} and V_{GS} in a similar way to that shown by the kink-related increase in I_D (more pronounced for higher V_{DS} and V_{GS}). However, the relative increase in $S_{ID}(0)$ with respect to its value when impact ionization is not considered in the simulations is much higher than that of I_D. Thus, although the kink effect in the I_D–V_{DS} curves is hardly detectable for the values of V_{DS} between 0.2 and 0.3 V (figure 2(*b*)), $S_{ID}(0)$ already exhibits a significant increase with respect to its value in the absence of impact ionization. For example, the relative increase in I_D when impact

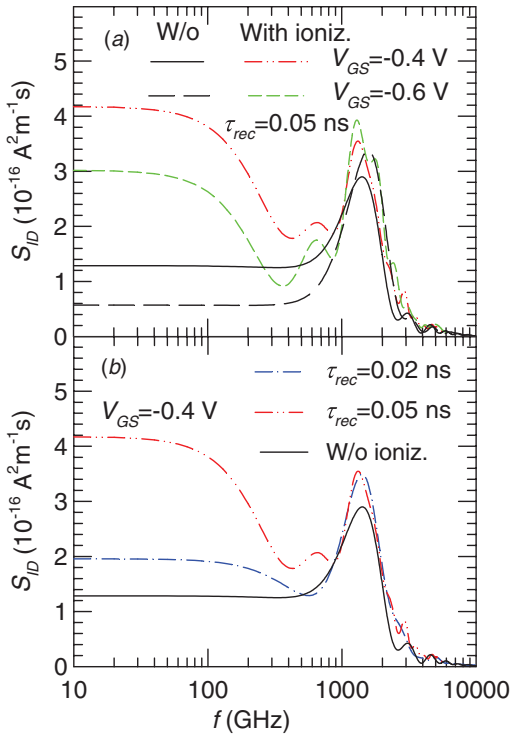

Figure 4. MC values of $S_{ID}(f)$ in the presence and absence of impact ionization, for (*a*) $V_{DS} = 0.4$ V, $\tau_{rec} = 0.05$ ns and different V_{GS}, and for (*b*) $V_{GS} = -0.4$ V, $V_{DS} = 0.4$ V and different τ_{rec}. $E_{th} = 0.41$ eV and $S = 10^{12}$ s^{-1}.

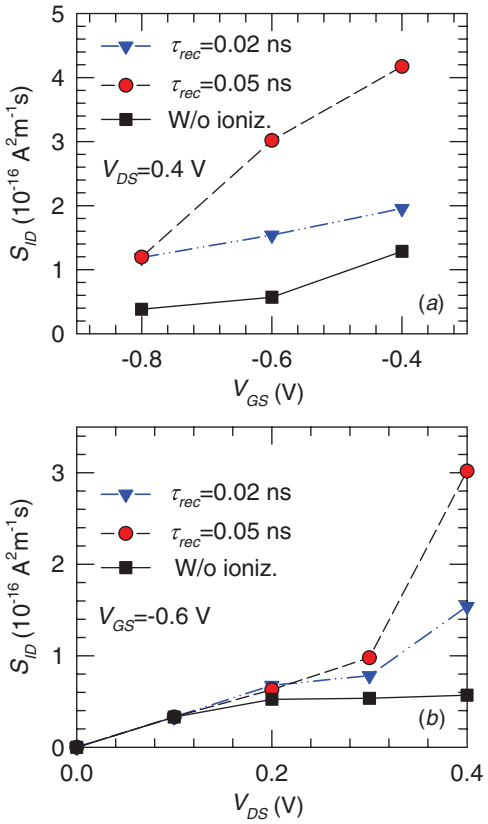

Figure 5. MC values of $S_{ID}(0)$ in the presence and absence of impact ionization, as a function of (*a*) V_{GS} being $V_{DS} = 0.4$ V and (*b*) V_{DS} being $V_{GS} = -0.6$ V. $E_{th} = 0.41$ eV, $S = 10^{12}$ s^{-1} and different τ_{rec}.

ionization takes place with respect to the case of the absence of impact ionization is about 12% for $V_{GS} = -0.6$ V, $V_{DS} = 0.3$ V and $\tau_{rec} = 0.05$ ns, while the increase in $S_{ID}(0)$ is around 83%. This indicates that when HEMTs are biased in the vicinity of the kink onset, even if the static behavior of the transistors is not strongly perturbed, their noise performance can be extremely degraded, since drain noise is very sensitive to the dynamics of holes generated by impact ionization. This fact further confirms that the increase in S_{ID} associated with the kink effect is mainly due to the appearance of an excess noise connected with the strong drain current fluctuations initiated by the variations of the hole concentration in the buffer.

4. Conclusions

We have presented an MC-based study of the degradation introduced by the kink effect in the noise performance of an isolated-gate InAs/AlSb HEMT. For this purpose, we have analyzed the drain current spectral density calculated by the Fourier transform of the drain current fluctuation correlation function. The fluctuations of the hole pile-up originated by impact ionization are linked to those of the drain current through the fluctuations of the potential barrier that controls the electron transport through the channel. As a consequence, the spectral density of the drain current presents a low-frequency plateau whose cutoff frequency is linked to the impact ionization rate and the hole recombination probability. The drain noise is very sensitive to the dynamics of holes generated by impact ionization; indeed, the noise performance of InAs/AlSb HEMTs can be seriously degraded when they are biased in the vicinity of the kink onset, even if the static behavior of the transistors is not perturbed.

Acknowledgments

This work has been partially supported by the Dirección General de Investigación (MICINN) through Project TEC2010-15413, by the Consejería de Educación, Junta de Castilla y León through Project GR270.

References

[1] Boos J B, Kruppa W, Bennett B R, Park D, Kirchoefer S W, Bass R and Dietrich H B 1998 AlSb/InAs HEMTs for low-voltage, high-speed applications *IEEE Trans. Electron Devices* **45** 1869

[2] Bolognesi C R, Dvorak M W and Chow D H 1999 Impact ionization suppression by quantum confinement: effects on the DC and microwave performance of narrow band-gap channel InAs/AlSb HEMTs *IEEE Trans. Electron Devices* **46** 826

[3] Kruppa W, Boos J B, Bennett B R, Papanicolaou N A, Park D and Bass R 2007 Low-frequency noise in AlSb/InAs and related HEMTs *IEEE Trans. Electron Devices* **54** 1193

[4] Ma B Y, Bergman J, Chen P, Hacker J B, Sullivan G, Nagy G and Brar B 2006 InAs/AlSb HEMT and its application to ultra-low-power wideband high-gain low-noise amplifiers *IEEE Trans. Microw. Theory Tech.* **54** 4448

[5] Kim D-H and del Alamo J A 2010 30-nm InAs PHEMTs with $f_t = 644$ GHz and $f_{max} = 681$ GHz *IEEE Electron Device Lett.* **31** 806

[6] Malmkvist M, Lefebvre E, Borg M, Desplanque L, Wallart X, Dambrine G, Bollaert S and Grahn J 2008 Electrical characterization and small-signal modeling of InAs/AlSb HEMTs for low-noise and high-frequency applications *IEEE Trans. Microw. Theory Tech.* **56** 2685

[7] Lefebvre E, Malmkvist M, Borg M, Desplanque L, Wallar X, Dambrine G, Bollaert S and Grahn J 2009 Gate-recess technology for InAs/AlSb HEMTs *IEEE Trans. Electron Devices* **56** 1904

[8] Mateos J, González T, Pardo D, Hoel V, Happy H and Cappy A 2000 Monte Carlo simulator for the design optimization of low-noise HEMTs *IEEE Trans. Electron Devices* **47** 1950

[9] Rodilla H, González T, Pardo D and Mateos J 2009 High-mobility heterostructures based on InAs and InSb: a Monte Carlo study *J. Appl. Phys.* **105** 113705

[10] Rodilla H, González T, Moschetty G, Grahn J and Mateos J 2011 Dynamic Monte Carlo study of isolated-gate InAs/AlSb HEMTs *Semicond. Sci. Technol.* **26** 025004

[11] Rodilla H, González T, Moschetty G, Grahn J and Mateos J 2012 Monte Carlo study of the noise performance of isolated-gate InAs/AlSb HEMTs *Semicond. Sci. Technol.* **27** 015008

[12] Vasallo B G, Mateos J, Pardo D and González T 2003 Monte Carlo study of the kink effect in short-channel InAlAs/InGaAs high electron mobility transistors *J. Appl. Phys.* **94** 4096

[13] Vasallo B G, Mateos J, Pardo D and González T 2004 Kink-effect related noise in InAlAs/InGaAs high electron mobility transistors *J. Appl. Phys.* **95** 8271

[14] Vasallo B G, Rodilla H, González T, Moschetty G, Grahn J and Mateos J 2010 Monte Carlo study of kink effect in isolated-gate InAs/AlSb high electron mobility transistors *J. Appl. Phys.* **108** 094505

[15] Fischetti V 1991 Monte Carlo simulation of transport in technologically significant semiconductors of the diamond and zinc-blende structures—part I: homogeneous transport *IEEE Trans. Electron Devices* **38** 634